

Lawrence Berkeley National Laboratory

Recent Work

Title

COMPLEX FRAGMENT EMISSION AT INTERMEDIATE ENERGIES

Permalink

<https://escholarship.org/uc/item/0bp4w5q8>

Author

Charity, R.

Publication Date

1987-04-01

c-2



Lawrence Berkeley Laboratory

UNIVERSITY OF CALIFORNIA

RECEIVED
LAWRENCE
BERKELEY LABORATORY

JUN 9 1987

LIBRARY AND
DOCUMENTS SECTION

Submitted to Nuclear Physics A

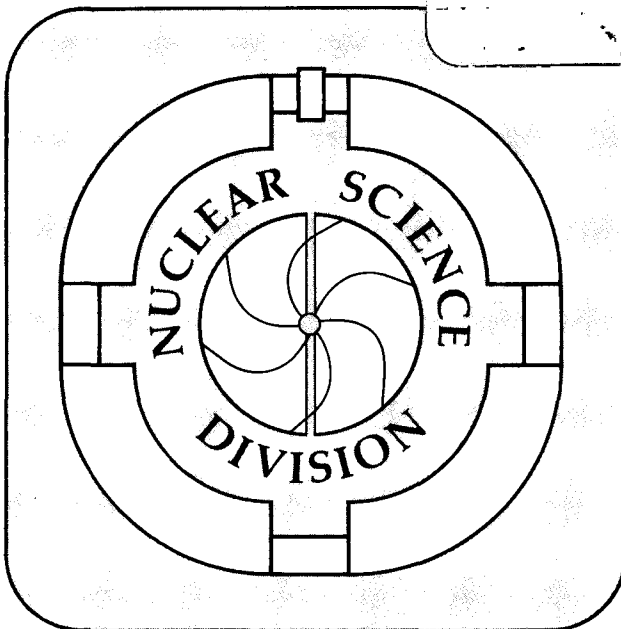
COMPLEX FRAGMENT EMISSION AT INTERMEDIATE ENERGIES

R. Charity

April 1987

TWO-WEEK LOAN COPY

*This is a Library Circulating Copy
which may be borrowed for two weeks.*



LBL-23332
c-2

DISCLAIMER

This document was prepared as an account of work sponsored by the United States Government. While this document is believed to contain correct information, neither the United States Government nor any agency thereof, nor the Regents of the University of California, nor any of their employees, makes any warranty, express or implied, or assumes any legal responsibility for the accuracy, completeness, or usefulness of any information, apparatus, product, or process disclosed, or represents that its use would not infringe privately owned rights. Reference herein to any specific commercial product, process, or service by its trade name, trademark, manufacturer, or otherwise, does not necessarily constitute or imply its endorsement, recommendation, or favoring by the United States Government or any agency thereof, or the Regents of the University of California. The views and opinions of authors expressed herein do not necessarily state or reflect those of the United States Government or any agency thereof or the Regents of the University of California.

LBL-23332

Complex Fragment Emission at Intermediate Energies

Robert Charity

Nuclear Science Division
Lawrence Berkeley Laboratory
University of California
Berkeley, California 94720

April 1987

This work was supported by the Director, Office of Energy Research,
Division of Nuclear Physics of the Office of High Energy and Nuclear Physics
of the U.S. Department of Energy under Contract DE-AC03-76SF00098.

COMPLEX FRAGMENT EMISSION AT INTERMEDIATE ENERGIES

Robert CHARITY

Nuclear Science Division, Lawrence Berkeley Laboratory, University of California, Berkeley, California, 94720

Complex fragment emission from the reactions Nb + Be, Al at $E/A = 8.4$ to 30.3 MeV and from La + C at $E/A = 50$ MeV/u have been detected. The dominant mechanism for the emission of the emission of fragment with $Z > 10$ is shown to be the statistical-binary decay of fusion-like products.

1. INTRODUCTION

Complex fragment or intermediate mass fragment emission has been observed both at low and high bombarding energies. At low bombarding energies ($E/A < 10$ MeV), complex fragment emission has been characterized as the statistical-binary decay of a classical compound nucleus formed in a complete fusion reaction (1,2). The yields of these fragments reflect the conditional barriers associated with the potential energy surface of the compound nucleus. In contrast, at much larger energies ($E/A > 100$ MeV), complex fragment mass yields follow power laws. The origin of these fragment has not been fully characterized at the present time, though they are usually thought to be associated with a multi-fragmentation production mechanism. In the intermediate energy regime one might expect to see a transition from the production of fragments by a binary decay mechanism to a multi-fragmentation mechanism.

In a series of experiments (3,4,5), we have studied complex fragment production at progressively larger bombarding energies. The energies studied range from 8.4 MeV/u to 50 MeV/u, which is the highest bombarding energy studied at present. In these experiments, we can follow the evolution of the statistical-binary decay products and look for the onset of multi-fragmentation or other binary production mechanisms.

Experiments were performed at the LBL SuperHILAC and Bevalac and the GSI Unilac. The experiments studied the asymmetric, reverse kinematics reactions Nb+Be, Al and La + C. The use of reverse kinematics confers a number of advantages for measuring complex fragments. Firstly, complex fragments are emitted with large laboratory energies, thus allowing easy detection and identification. This is in contrast to normal kinematics, where the heavier fragments are emitted with very small energies, typically below the detector

thresholds. Reverse kinematics is thus particularly suitable for studying the heavier complex fragments.

Because of the strong forward focusing in the reverse kinematics, the differential cross sections are greatly increased in the laboratory frame. Thus, one needs only modest sized detectors to obtain reasonable yields even when the total cross sections are very low. The experiments were performed with two Gas-Si, E- Δ E telescopes positioned at very small angles on either side of the beam. The telescopes were position sensitive in both the x and y directions and each covered an angular range of approximately 5°. The minimum angle at which particles were detected was typically 3°.

2. RESULTS AND DISCUSSION

In Fig. 1. we show the contours of the invariant cross section in the

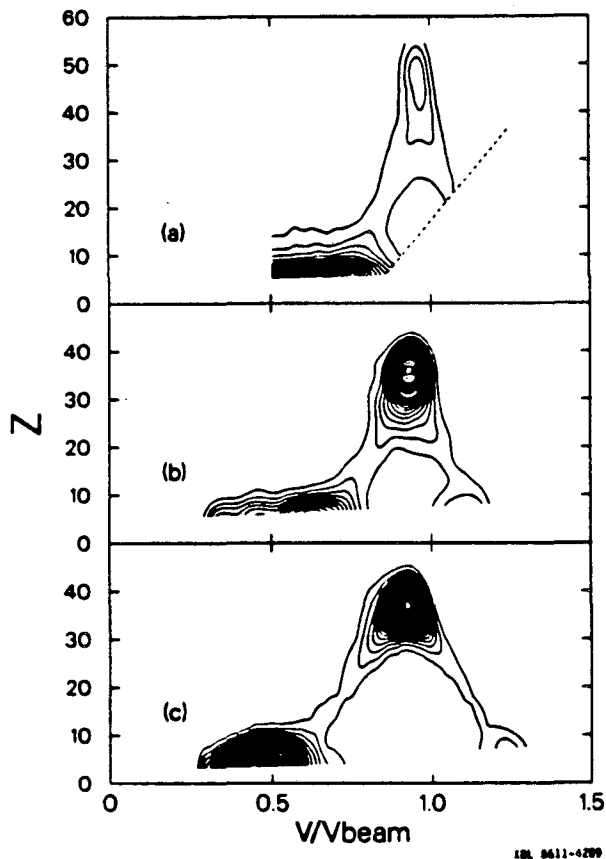


FIGURE 1

Singles distributions of reaction products plotted as linear contours of invariant cross section in the velocity-Z plane for three different reactions: a) 50 MeV/u $^{139}\text{La} + ^{12}\text{C}$ for laboratory angles from 3° to 8°. The dashed line is an experimental threshold for particles which punch-through the telescope; b) 30.3 MeV/u $^{93}\text{Nb} + ^9\text{Be}$ for angles from 4° to 10°; and c) 17.7 MeV/u $^{93}\text{Nb} + ^9\text{Be}$ at an angle of 4.6°.

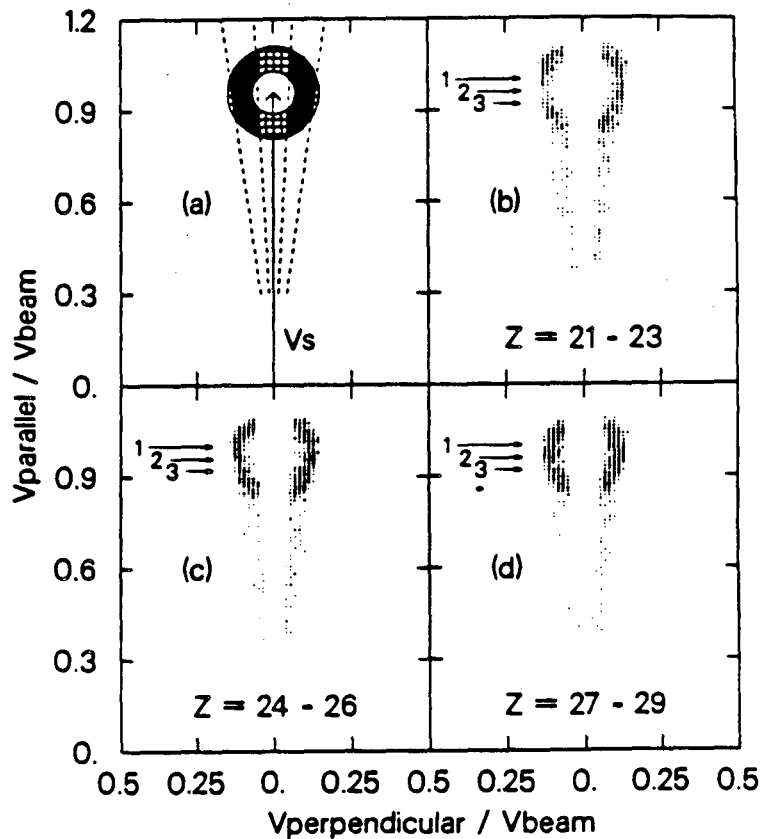
Z-velocity plane for three reactions with bombarding energies from 18 to 50 MeV/u. In all of these reactions we see the same three components. Firstly,

for Z-values near the projectile value, we see a large yield associated with evaporation residues. These results from the decay of complete or incomplete fusion-products. This component is only seen at the very forward angles.

Emerging from the base of the evaporation residues are two distinct ridges. These represent the two kinematic solutions associated with the binary decay of a fusion-like residue. A high velocity solution corresponding to emission of a fragment forward in the center-of-mass and a low velocity solution corresponding to emission backward in the center-of-mass.

There is a third component seen at low velocities and with Z-values similar to the target value. This component may be due to some type of quasi-elastic interaction and is the analog of the high velocity complex fragments observed at forward angles in normal kinematics.

In the rest of this work we will concentrate on the second of these components, showing it results from the statistical decay of hot fusion-like products. The binary nature of this component is shown very clearly in plots shown in Fig.2 b,c&d obtained with the 50 MeV/u La + C reaction. In these



LBL 8611-4288

FIGURE 2

(a) Schematic representation of the invariant cross section in the V_{\parallel}, V_{\perp} plane for complex fragment emission from a compound nucleus with a well defined velocity, V_s . The Coulomb circle is the locus of events smeared out by sequential evaporation. The geometric limits of the detector are shown by the dashed lines and the solid area is the predicted experimental distribution; (b,c,d) Experimental distributions for various Z bins.

density plots of the invariant cross sections in the $V_{\parallel}-V_{\perp}$ plane, complex fragments lie on what we call a Coulomb circle. The outer portions of this circles are clearly observed in Figs. 2 b, c&d. The inner portion is missing due to the limited angular coverage of the detectors. The radii of the Coulomb circle become larger with decreasing complex fragment Z-value. The origin of these Coulomb circle is illustrated by the schematic kinematics diagram shown in Fig 2a. A fast moving source system, with velocity vector V_s , decays by binary division into complex fragments. The complex fragments are emitted with a velocity determined largely by the Coulomb repulsion between the two nascent fragments. Thus, each complex fragment Z species lie on a circle, centered around the arrow head of the source vector, with a radius equal to the fragment's Coulomb velocity. Note that the existence of Coulomb circles implies the fragments were formed in a binary decay. In a multi-fragmentation event, where three or more large fragments are produced, each Z species will no longer have a well defined emission velocity. This will result in a filling in of the Coulomb circles.

The binary character of these complex fragments events is also seen in coincidence measurements. Fig. 3 shows the $Z_1 - Z_2$ correlation plot of

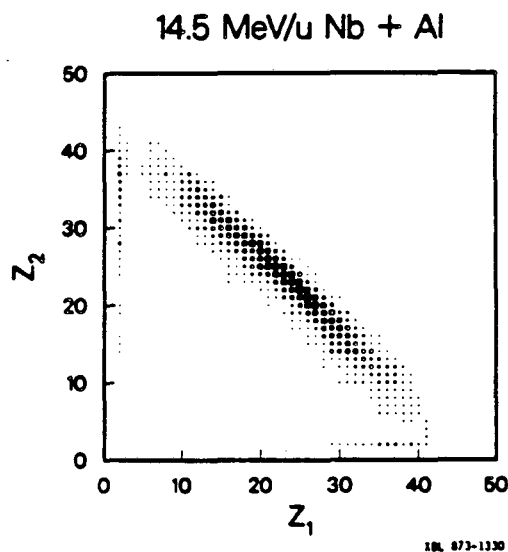


FIGURE 3

Scatter plot of the experimental Z correlation for coincidence events detected in the reaction 14.4 MeV/ Nb + Al. Z_1 fragments were detected at angles from 4° to 9° and Z_2 fragments from -4° to -9° .

coincidence events in two telescopes either side of the beam axis for the reaction 14.5 MeV/u Nb + Al. Most of the events lie in a band corresponding to $Z_1 + Z_2$ being approximately constant. The average values of Z_1+Z_2 for this reaction is 47, which is a large fraction of the total charge in this

reaction, $Z_p + Z_t = 54$. Of course one may not see the total Z of the original source system due to the inevitable sequential evaporation of light particles from the hot primary fragments. Thus the complex fragments in this reactions result from the binary breakup of some system with $Z \geq 47$. Fig. 4 shows a correlation plot for the reaction 50 MeV/u La + C. The band of the

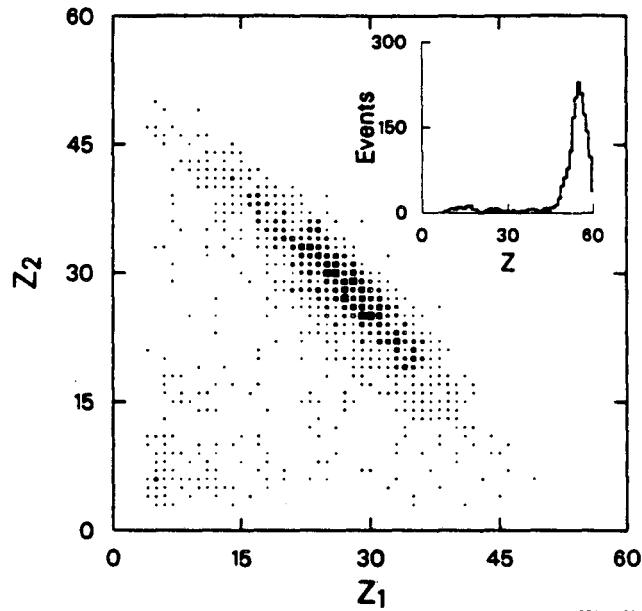


FIGURE 4

As in Fig. 3, now for the reaction 50 MeV/u La + C. The inset shows the distribution of the sum of charges ($Z = Z_1 + Z_2$).

binary events is again clearly visible, with an average values of $Z_1 + Z_2$ equal to 55. This represents a similar fraction of the total reaction charge ($Z_p + Z_t = 63$). One is also just starting to see some events where the two coincident fragments represent only a small fraction of $Z_p + Z_t$. Presumably, these represent some higher multiplicity events. However, their cross section is very small relative to the binary events.

In all of the systems studies, the velocity spectra and coincidence data point to a binary production mechanism for the complex fragments of charge intermediate between the target and projectile Z -values. This is similar to results we obtained at lower bombarding energies, where complex fragments could be characterized as the decay products of compound nuclei produced in complete fusion reactions. At these higher bombarding energies, it is interesting to see whether the intermediate source system, which emitted the fragments, obtained full relaxation. A necessary requirement of full relaxation is the backward-forward symmetry of the angular distributions. Fig. 5 shows the angular distribution, in the center-of-mass of the source system, for $Z=20$ fragments produced in the reaction 17.7 MeV/u Nb + Be. The

shape of the angular distribution is symmetric about 90 degrees and follows the $1/\sin\theta$ dependence shown the dashed line. A $1/\sin\theta$ form of the angular distribution is expected for decay from a rapidly rotating system. For most complex fragment, our experimental coverage of laboratory angle did not correspond to such a large coverage of center-of-mass angle as in Fig. 5.

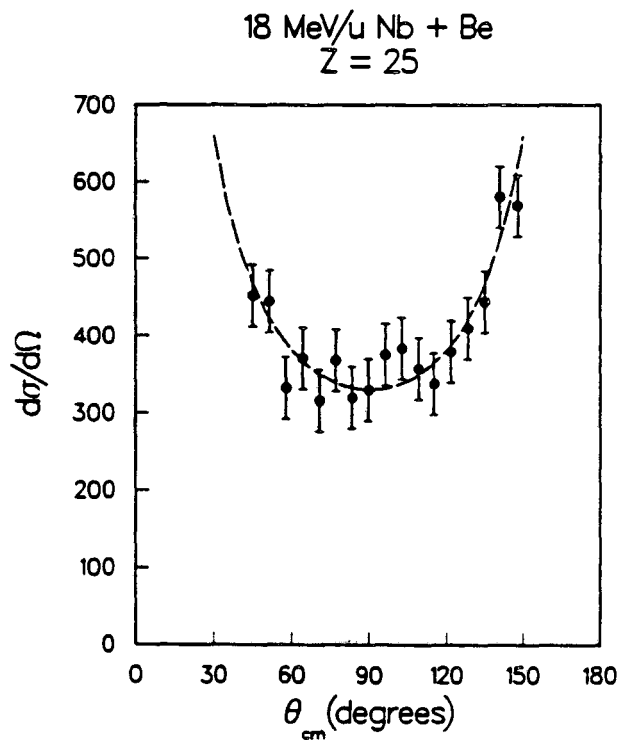


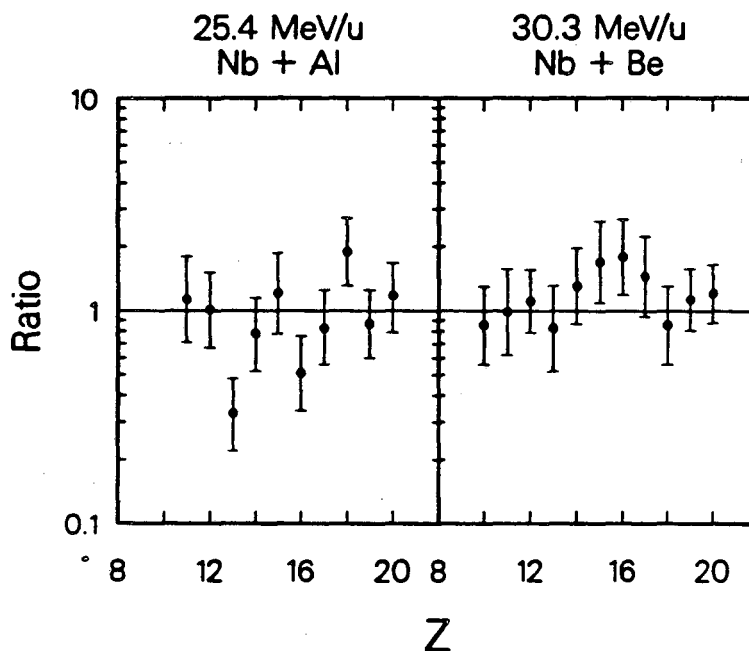
FIGURE 5

Experimental Angular distribution of $Z=20$ fragments in the center-of-mass frame of the source system for the reaction $17.7 \text{ Nb} + \text{Be}$. The dashed curve shows an angular distribution with a $1/\sin\theta$ dependence fitted to the data.

However we can still gauge the backward-forward symmetry of the angular distributions from the yields of the high and low velocity kinematic solutions, which correspond to emission forward and backward in the center-of-mass. In Fig. 6 we show the ratio of $\partial^2\sigma/\partial Z\partial\theta$ for the high and low velocity kinematic solutions plotted as a function of fragment Z -value for two Nb induced reactions. The experimental point are consistent with a ratio of unity, which corresponds to a $1/\sin\theta$ angular distributions. The angular distribution thus imply a high degree of relaxation obtained by the intermediate source system. Of course the most stringent test of full relaxation is to see whether the complex fragment cross sections are consistent with statistical model branching ratios. We will get back to this point latter.

One piece of information readily extracted from the Coulomb circles is the source velocities. These relate directly to the momentum transfer associated

with the reactions. In Fig 7. we show source velocities obtained in the



XBL 873-1333

FIGURE 6

Ratios of $\sigma^2/\sigma\sigma Z$ between the high and low velocity kinematic solutions as a function of Z . A ratio of unity indicates a $1/\sin\theta$ form of the angular distribution.

reactions Nb + Be & Al at $E/A = 14.4$ and 17.7 MeV. The first point, to be drawn from this figure, is that the source velocities are independent of the fragment Z -value. This suggest that the fragments were all emitted from a common source. Secondly, there is no change in the source velocities between the 14.4 and 17.7 MeV/u bombarding energies. The source velocities are expected to fall somewhere between the beam velocity, which corresponds to zero momentum transfer, and the velocity associated with complete fusion which, of course, correspond to complete momentum transfer. Note we use "momentum transfer" in the same context that would be used in the equivalent normal kinematics reactions. In these reverse kinematics reactions we essentially always have complete momentum transfer. The dashed lines in Fig.7 indicate the complete fusion velocity for these reactions. Our data lie just above this line indicating almost complete momentum transfer. We can contrast this to the source velocities shown in Fig. 8, obtained in the reaction La + C at the higher bombarding energy of $E/A=50$ MeV. Here the source velocities are significantly larger than the complete fusion velocity. They lie about about half way between this velocity and the beam velocity. In this case we are seeing about 50% momentum transfer. The complex fragments thus are emitted from compound systems which are formed in complete fusion reactions at low bombarding energies and via incomplete fusion reactions at the larger

bombarding energies.

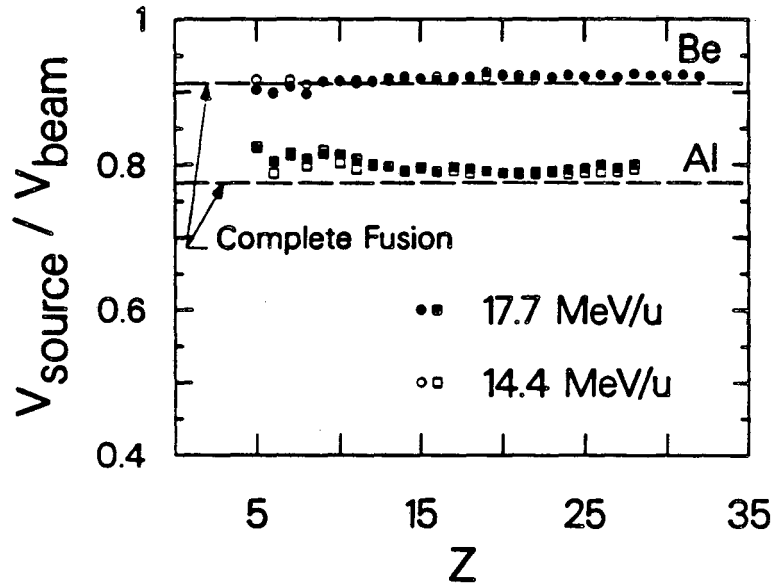


FIGURE 7

Measured source velocities plotted as a function of fragment Z-value for the systems 14.5, 17.7 MeV/u Nb + Be, Al. The dashed lines are the velocities corresponding to complete fusion of the target and projectile.

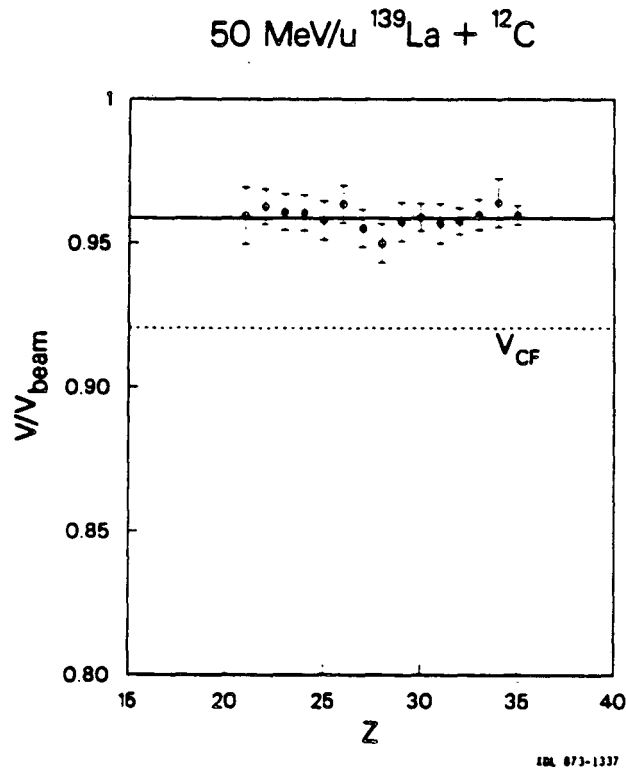


FIGURE 8

As in Fig. 7, now 50 MeV/u La + C.

Fig. 9 shows the velocity at which the fragments were emitted from the

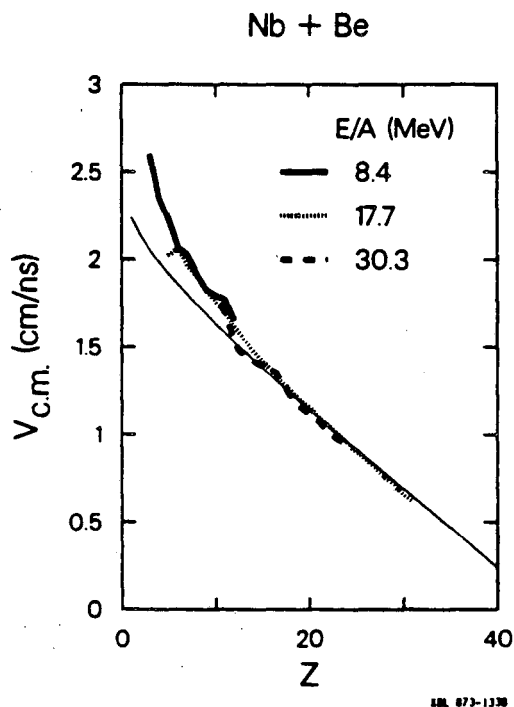
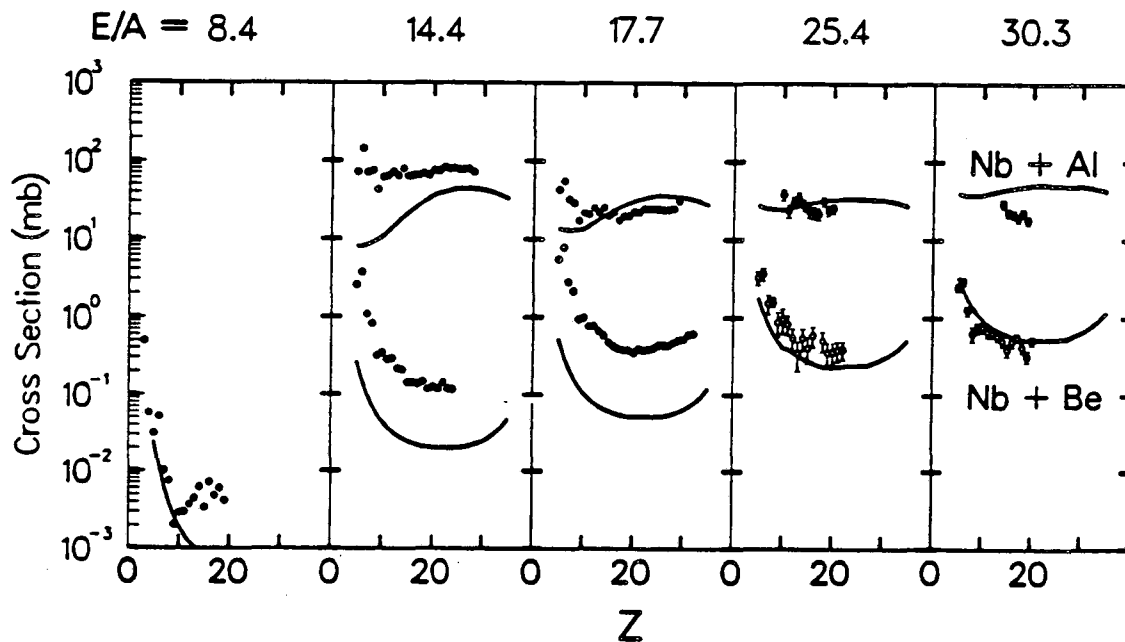


FIGURE 9

Velocities of fragments in the center-of-mass of the source systems extracted from the reactions 8.4, 17.7 and 30.3 MeV/u Nb + Be. The thin solid curve shows a calculation of the velocities estimated from the Coulomb repulsion of two spheres.

source system, for Nb + Be reactions at various bombarding energies. These were obtained from the radii of the Coulomb circles. Note there is very little change in these velocities from 8 to 30 MeV/u. This is not unexpected, because of the small Z of the Be target. The total charge of the fusion-like product formed in these reactions varies little with the degree of incomplete fusion. Thus the Coulomb velocities are not expected to change greatly with bombarding energy. We have compared the experimental data in Fig. 9 to Coulomb velocities derived from the Viola systematics of fission kinetic energy. The thin solid curve represents a calculation, assuming charge equilibration in each mass split, obtained from these systematics. This curve is in excellent agreement with the data except for the very asymmetric splits where charge equilibration is not expected not hold. In this region, the lighter fragments are expected to have a charge to mass ratio closer to that of the beta line of stability, which would result in larger emission velocities.

For the reactions Nb + Be & Al, we have studied the complex fragment decay over a large range of bombarding energies. The evolution of the fragment charge distributions with bombarding energy is shown in Fig. 10. The shapes



XBL 873-1329

FIGURE 10

Angle-integrated cross sections for complex fragments associated with the statistical-binary decay mechanism for various Nb + Be, Al reactions with bombarding energies from 8.4 to 30.3 MeV/u. The solid curve shows the results of statistical model calculations of these cross sections.

of the charge distributions are easily understood in terms of the statistical model. The $A \approx 100$ systems we are forming in the Nb + Be reactions, have a fissility below the Businaro-Gallone point. The conditional fission barriers as a function of the asymmetry of the split have a maximum for symmetric division. This corresponds to a minimum in the yield. The charge distributions for Nb + Be reactions do exhibit a minimum for symmetry division ($Z \approx 22$). For the Nb + Al reactions, one forms heavier compound systems and with the larger angular momenta expected these reactions, the effective fissility will be much closer to the Businaro-Gallone point. This is reflected in the much flatter charge distributions compared to the Nb + Be reactions. The variation of the cross sections with bombarding energy is quite interesting. For the Nb + Be reactions, the cross sections increase quite rapidly up to 18 MeV/u after which they remain relatively constant. For the Nb + Al reaction, the cross sections actually decrease from 14 to 18 MeV/u, after which they are also relatively constant. We have recently starting calculating cross sections in these reactions using the statistical model. One particular problem in such calculations, is determining the initial Z, A, E^*, J distributions of compound nuclei produced in the incomplete fusion reactions. In lieu of any

experimental guidance, we have used an abrasion model developed by Moretto (6), to derive the initial distributions. For a given impact parameter, either occluded volumes of the two overlapping spheres may be sheared away in the collision. The energy of the newly created surfaces as well as the inertias of the relative pieces determine which of the two occluded pieces are sheared. For asymmetric systems, the smaller nucleus will bear the brunt of the shearing, as it involves the creating a smaller surface area. The sheared off piece will then amalgamate with the intact nucleus, forming an incomplete fusion product. In the reactions of interest here, this model predicts complete fusion for small impact parameters associated with complete overlap. For progressively larger impact parameters, complete fusion still occur for partial overlap until a critical value where shearing is first possible. At the critical values there is sharp drop in the transferred angular momenta and the excitation energy of the fusion-like product. An example of the predicted excitation energies and transferred angular momenta of fusion-like products is shown in Fig. 11.

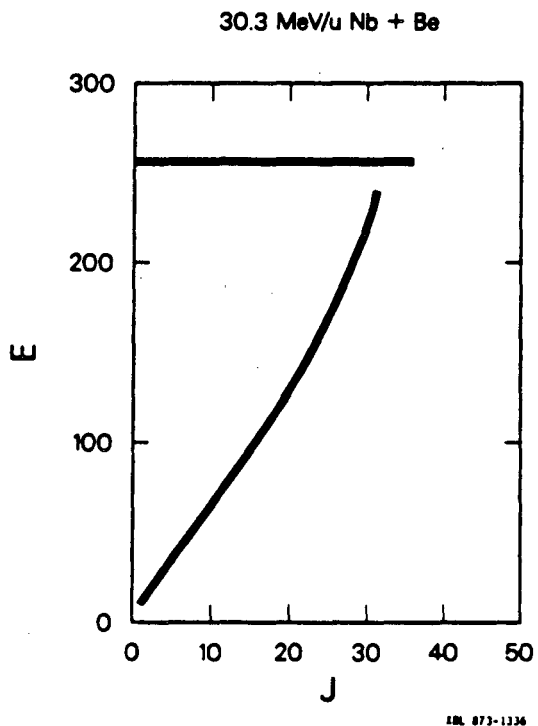


FIGURE 11

Example of the excitation energy and transferred angular momentum of fusion-like products used in the statistical model calculations.

Cross sections were calculated, from such initial populations, with the statistical model using the transition state formalism of Moretto (7) for complex fragment production. The expression for the decay width associated

with the binary decay of a system into the fragments Z_1, A_1 and Z_2, A_2 can be approximated to

$$\Gamma(Z_1, A_1, Z_2, A_2) = T/2\pi\rho(E^*, J) \rho^*(E^* - E_{\text{sad}}(Z_1, A_1, Z_2, A_2, J), J)$$

where ρ and ρ^* are the level densities of the compound nucleus and at the conditional saddle point, E_{sad} is the deformation plus rotation energy of the conditional saddle point configuration and T is the saddle point temperature. The Finite Range Model gives excellent reproduction of the experimental asymmetric barriers in the $A \approx 100$ region (8). As these barriers were unavailable at present for the systems of interest in this work, we have used saddle point energies (E_{sad}) calculated from liquid drop model barriers scaled so as to reproduce the Finite Range Model predictions for symmetric division. After comparing such barriers for ^{110}In to the Finite Range barriers calculated by Sierk (8), we expect the barriers we used to be too large for the very asymmetric mass splits.

Because of the large excitation energies associated with these reactions, multi-chance emission of fragments will be an important effect. We have therefore used the statistical model code PACE to calculate the E^*, J populations of intermediate systems produced in the decay of an initial compound nucleus by light particle evaporation. Complex fragment cross sections associated with each of these intermediate systems were calculated using the total decay width predicted by PACE.

Fig. 12 shows some results of these calculations. The predicted cross sections for emitting a $Z=20$ fragment somewhere in the decay process, is plotted for each entrance L-wave. For the Nb + Be reaction, this cross section increased rapidly with the increasing L-wave (The larger transferred angular momenta lower the conditional barriers) until the critical impact parameter is reached after which incomplete fusion occurs. The sharp drop in the complex fragment decay probability is due to the sharp drop in the transferred angular momentum and excitation energy at the onset of incomplete fusion. For the Nb + Be reaction, incomplete fusion products are predicted to produce only a small fraction of the total complex fragment yield.

In contrast, for the Nb + Al reaction, there is also a sharp drop in the cross section at the onset of incomplete fusion, but the cross section then increases at the higher L-waves. Incomplete fusion products are predicted to be associated with the majority of the complex fragment yield in this reaction.

The calculated complex fragment cross sections are compared to the experimental data in the Fig. 10. Considering the many assumptions in these calculations, our ability to reproduce the experimental data to within a

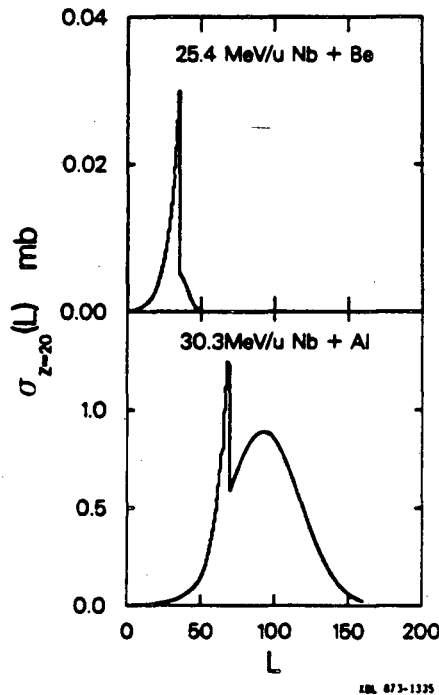


FIGURE 12

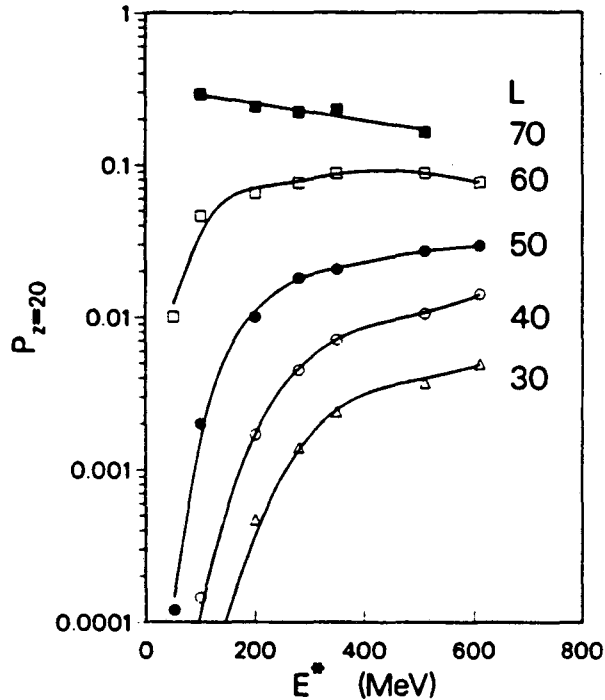
Predicted cross sections for $Z=20$ fragments associated with each entrance channel L -wave.

factor of 10 is very encouraging. The agreement between experiment and the calculations is indeed much better at the higher bombarding energies where we expect the incomplete fusion abrasion model to be more applicable. For the 8.4 MeV/u Nb + Be data, we can obtain excellent agreement with the experimental data using the E^*, J initial distributions of compound nuclei predicted by conventional fusion models, such as the Bass model. This underlies a problem with the abrasion model in that it ignores the effects of the potential energy, which is well known to play a paramount role at the lower energies, but should become less important with increasing energy.

In the 30.3 MeV/u Nb + Al reaction, complete fusion would result in 610 MeV of excitation energy. One would expect pre-equilibrium processes to be important in this case. However, this may not have that large an effect on the predicted cross sections.

In Fig. 13 we show the total probability of emitting a $Z=20$ fragment as a function of the excitation energy and angular momentum. Our calculations predict most of the cross sections results from the largest transferred angular momenta, which are around 60 \hbar . For such angular momenta, the decay probability is quite insensitive to the excitation energy. A large amount of excitation energy can be lost to pre-equilibrium processes without greatly effecting the predicted cross sections. For Nb + Be reactions, where

Z=54 A=120



XBL 873-1328

FIGURE 13

The predicted probability of emitting a Z=20 fragment in the decay chain of the system Z=54, A=100 as a function of initial excitation energy. The curves show the results for various initial transferred angular momenta.

most of the complex fragment yield comes from angular momenta around 30 \hbar , the cross sections are more sensitive to pre-equilibrium processes.

In spite of the many uncertainties associated with these calculations, they predict the general dependence of the cross sections on bombarding energy and the large difference in cross section between the Be and Al induced reactions. We thus conclude that the cross sections are consistent with statistical model branching ratios, and thus the fusion-like products obtained full relaxation.

In the statistical model calculations, complex fragment emission is not the dominant decay mechanism even at the highest excitation energies. Most fusion-like products are expected to decay solely by light particle emission resulting in evaporation residues. We see a small fraction of these evaporation residues in our detectors (Fig. 1), however they are found only at very forward angles in these reverse kinematics reactions.

3. SUMMARY

In conclusion, we have shown that the statistical-binary decay of fusion-like products is still an important production mechanism of complex

fragments for bombarding energies up to 50 MeV/u. This mechanism accounts for all the fragments with $Z > 10$. For fragments with $Z < 10$, in addition to the statistical-binary decay we also observe another component which may arise from some quasi-elastic type of interaction. For the systems studied, there is no evidence of any appreciable amount of multi-fragmentation.

For bombarding energies up to 50 MeV/u, fully relaxed systems are still formed in fusion-like reaction. The excitation energy of these system can be quite large ($E^*/A > 4$ MeV). The emission complex fragments from such systems offers an opportunity to study the properties of nuclei as their excitation energies approaches the total nuclear binding energy.

ACKNOWLEDGMENT

This work was supported by the Director, Office of Energy Research, Division of Nuclear Physics of the Office of High Energy and Nuclear Physics of the U.S. Department of Energy under Contract DE-AC03-76SF00098.

REFERENCES

- 1) L.G. Sobotka, M.L. Padgett, G.J. Wozniak, G. Guarino, A.J. Pacheco, L.G. Moretto, Y. Chan, R.G. Stokstad, I. Tserruga, and S. Wald, Phys. Rev. Lett. 51 (1983) 2187.
- 2) M.A. McMahan, L.G. Moretto, M.L. Padgett, G.J. Wozniak, L.G. Sobotka, M.G. Mustafa. Phys. Rev. Lett. 54 (1985) 1995.
- 3) L.G. Sobotka, M.A. McMahan, R.J. McDonald, C. Sigarieux, G.J. Wozniak, M.L. Padgett, J.H. Gu, Z.H. Liu, Z.Q. Yao and L.G. Moretto. Phys. Rev. Lett. 53 (1984) 2004.
- 4) R.J. Charity, M.A. McMahan, D.R. Bowman, Z.H. Liu, R.J. McDonald, G.J. Wozniak, L.G. Moretto, S. Bradley, W.L. Kehoe, A.C. Mignerey, and M.N. Namboodiri, Phys. Rev. Lett. 56 (1986) 1354.
- 5) D.R. Bowman, R.J. Charity, R.J. McDonald, M.A. McMahan, G.J. Wozniak, L.G. Moretto, W.L. Kehoe, S. Bradley, A.C. Mignerey, A. Moroni, A. Bracco, I. Iori, and M.N. Namboodiri. To be published in Phys. Lett.
- 6) L.G. Moretto, Proceeding of the XVIII Mikolajki Summer School on Nuclear Physics, Mikolajki, Poland, Sept. 1986, LBL-21998.
- 7) L.G. Moretto, Nuc. Phys. A247 (1975) 211.
- 8) A. Sierk, Phys. Rev. Lett. 55 (1985) 582.

This report was done with support from the Department of Energy. Any conclusions or opinions expressed in this report represent solely those of the author(s) and not necessarily those of The Regents of the University of California, the Lawrence Berkeley Laboratory or the Department of Energy.

Reference to a company or product name does not imply approval or recommendation of the product by the University of California or the U.S. Department of Energy to the exclusion of others that may be suitable.

*LAWRENCE BERKELEY LABORATORY
TECHNICAL INFORMATION DEPARTMENT
UNIVERSITY OF CALIFORNIA
BERKELEY, CALIFORNIA 94720*